Molecular-orbital cluster-model study of the core-level spectrum of CO adsorbed on copper

P. S. Bagus and M. Seel
IBM Research Laboratory, San Jose, California 95193 and Lehrstuhl für Theoretische Chemie, Friedrich-Alexander-Universität Erlangen-Nürnberg, D-8520 Erlangen, West Germany
(Received 8 September 1980)

We have used *ab initio* self-consistent-field wave functions for a Cu_5CO cluster to model the interaction of CO with a Cu surface and to study the x-ray photoemission (XPS) from CO core levels. In order to justify the use of this cluster model of the chemisorption of CO on Cu, we show that we obtain reasonable values for the ground-state Cu—CO bond distance and bond strength and accurate values for the CO core-level ionization potentials. An extensive analysis of the initial-state chemical bonding and the final-state relaxation processes is given. We show that two types of final C_{1s} or O_{1s} core hole states exist with comparable photoionization intensities. The lowest state is a shakedown state in which a Cu 4*sp* valence electron is transferred to the CO $2\pi^*$ level effectively screening the core hole. The higher-lying final state closely resembles a "normal" one-hole core ion in which the metal electrons participate in the screening in only a very limited way. Our analysis shows that the intensity distribution between these two states is closely related to the extent of $2\pi^*$ backbonding in the unionized ground state of the system. We consider also the effects of spin coupling of the core hole to the $2\pi^*$ electron for the shakedown states. The existence of these two types of relaxed final states, shakedown and normal, is responsible for the broad core-level peaks observed in XPS spectra. This conclusion, based on a molecular-orbital analysis is similar to that reached by Schönhammer and Gunnarsson who used a parametrized Anderson-type Hamiltonian to describe the CO—Cu interaction.

I. INTRODUCTION

X-ray photoelectron spectroscopy (XPS) is used to study the chemical state and to obtain information about chemical bonding in a wide variety of materials. An especially important application is to the study of the bonding of chemisorbed species on surfaces; here XPS is particularly useful because of its high surface sensitivity. In general, multiple (or broad) core-level peaks in XPS spectra have been interpreted as being due to the presence of more than one chemical state of the element.[1] For an adsorbed species, such different states could arise, for example, from simultaneous molecular and dissociative chemisorption or from adsorption at different sites on the surface. However, there is now strong evidence that the XPS core level spectra of molecules adsorbed on metal surfaces may be broad and have a multipeak structure even though only one adsorption state is present.

Fuggle *et al.*[2] have compared the adsorbate XPS core line shapes and positions for several molecules on metal surfaces. Their comparison shows that weakly chemisorbed species [e.g., N_2 on Ni(100) and CO on Cu(100)] have broad and complex spectra while for physisorbed or strongly chemisorbed molecules the spectra have a simpler structure and consist of a dominant peak possibly with weak satellites. The first theoretical interpretation of this behavior was given by Schönhammer and Gunnarsson[3–5] (SG) who used an Anderson-type Hamiltonian to study the final-state response, or relaxation, to the adsorbate core hole. They ascribed the structure at lower binding energy to final relaxed states where a metal electron filled an adsorbate level which was empty in the initial state. This results in a screening of the core hole and a lowering of the total energy. The structure at higher binding energy is ascribed to states where the substrate electrons do not participate in the core hole screening, "unscreened states." In particular, SG have been able to reproduce[4] the multipeaked C_{1s} structure observed for CO on Cu(100).[2] However, it was necessary for them to use and to adjust empirical parameters to represent the adsorbate-substrate interaction in both the initial and final states.

Linear clusters[6,7] NiCO and NiN_2, have been used to model and study the adsorbate core level structure for CO on Ni and N_2 on Ni. Here, the properties of the adsorbate-substrate interaction were obtained directly from *ab initio* molecular-orbital (MO), self-consistent-field (SCF) wave functions for initial (unionized) and final (core-ionized) states, no adjustable parameters were required or used. Two kinds of cluster final states were obtained corresponding to the "screened" and "unscreened" states described by SG. Moreover, the distribution of intensity between these two states could, in the cluster model work, be simply related to the extent of the metal atom $4p$ to adsorbate $2\pi^*$ backbonding. When the backbonding was small, which occurred at large metal-adsorbate distances, the intensity of the screened state was small and that of the higher-binding-energy unscreened state was large. This corresponds to the case of physisorption. When the backbonding was large, corresponding to strong chemisorption, the reverse distribution of intensity was found. However, for these small clusters an excited state was used for the initial "ground state." This was necessary in order to have metal valence character which could interact with the adsorbate $2\pi^*$ level; in other words, in order to model the backbonding which may actually occur for the metal surface.[6–8]

In this paper, we report the results of a larger cluster model study of the XPS spectra for CO on Cu(100) based on *ab initio* MO SCF wave functions for a Cu_5CO cluster. CO in a $C(2\times2)$ overlayer structure on Cu(100) occupies a head-on adsorption site[9,10] and the Cu_5 cluster was chosen to model this site. Various properties of the ground state of Cu_5CO, including binding energy and equilibrium Cu–C distance, are consistent with experimental values.[10,11] Moreover, we find that the absolute ionization potentials (IP's) obtained from SCF calculations[12] for Cu_5CO are in remarkably good agreement with values observed for CO on Cu(100).[2,13] This makes it reasonable to expect that the Cu_5CO cluster is sufficiently large to properly represent the adsorbate-substrate interaction at a semiquantitative level or better for some purposes. Here, as for the one metal atom clusters,[6,7] we find both screened and unscreened final states. However, for Cu_5CO, there is no need to introduce an artificial ground state. We find that the metal valence ($4sp$) to $CO(2\pi^*)$ backbonding which occurs naturally for the true cluster ground state is sufficient to give relative final-state intensities which are in qualitative agreement with experiment.[2,13]

The present results provide strong new support that the origin of the complex adsorbate XPS structure is indeed due to screened and unscreened final states. This support is particularly important in that it is obtained from work which contains no adjustable parameters and with an approach which is completely different from that used by SG.[3–5]

In Sec. II, we describe the geometry of the Cu_5CO cluster and give some details of the SCF calculations. In Sec. III, we summarize some key properties of the bare, Cu_5, and adsorbate, Cu_5CO, cluster ground states. The ground-state results will be presented in more detail elsewhere.[14] A detailed analysis of the results for the adsorbate core ionized states, including a description of the electronic structure and the relative intensities of different final states, is presented in Sec. IV. Our conclusions are summarized in Sec. V.

II. COMPUTATIONAL DETAILS

The Cu_5 cluster is chosen to model a head-on adsorption site on an unrelaxed and unreconstructed Cu(100) surface. The first (surface) layer contains one atom, denoted Cu_1, and the second layer the four equivalent nearest neighbors of Cu_1, denoted Cu_2. The Cu_1–Cu_2 distance, 4.80 bohrs, is the bulk crystal distance.[15] The point-group symmetry of Cu_5 is C_{4v}. CO approaches normal to Cu_1 so that the Z axis of the cluster coincides with the CO internuclear axis; the point group of Cu_5CO is also C_{4v}. The C–O distance is fixed at 2.173 bohrs; this is the experimental value for $Ni(CO)_4$ (Ref. 16) and is also the distance determined by a low-energy electron diffraction (LEED) analysis[10] for CO on Cu(100) $C(2\times2)$. It is also quite close to the equilibrium internuclear distance in free CO, 2.132.[17] The Cu–C distance, $R(Cu_l\text{–}C)$, has been varied between 3.25 and 4.00 bohrs. This range includes the Cu–C distance determined by LEED to be 3.6 ± 0.2 bohrs.[10] The Cu_5CO cluster is shown schematically in Fig. 1.

All electron Hartree-Fock SCF wave functions have been determined for the ground state of the Cu_5 and Cu_5CO clusters and for several states involving core level ions of the C and O atoms. The SCF calculations were performed using extended basis sets of contracted Gaussian-type functions, CGTO's. For Cu, a $12s, 9p, 5d$ GTO basis set was contracted to

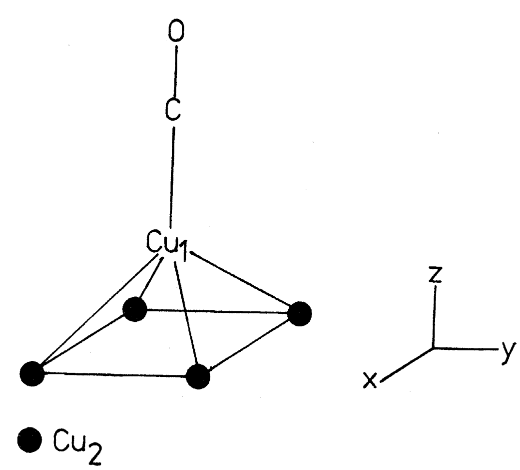

FIG. 1. Schematic representation of the Cu_5CO cluster.

$6s$, $5p$, $3d$. In order to reduce the magnitude of the calculation, the Cu basis set was contracted so that the Ne core orbitals were represented by a minimal basis. The $3s$, $3p$, $4s$, and $4p$ atomic shells were represented by a double zeta and the $3d$ shell by a triple zeta basis. The C and O basis sets were $9s$, $5p$ contracted to $4s$, $3p$.[18,19] These basis sets are sufficient to give reasonably accurate SCF results for the clusters.[19] In particular, the two $4p$ basis functions on Cu are required in order to permit $4p$ participation in the Cu "valance band" and in the bonding to CO. For the Cu_5 and Cu_5CO ground states, the SCF calculations were performed using C_{4v} symmetry and with spatial and spin-symmetry equivalence restrictions imposed.[20] For the ionic states, the spatial equivalence restriction was not imposed on the MO's: the reasons for this will be explained in Sec. IV.

III. GROUND-STATE PROPERTIES FOR Cu_5 AND Cu_5CO

The ground state of Cu_5 was determined to be a ^2E state with the configuration

$$17a_1^2\,11b_1^2\,18e^3 5b_2^2\,4a_2^2 \ , \qquad (1)$$

where only the highest occupied MO of each symmetry is indicated. The $17a_1$ and $18e$ orbitals are composed predominantly of $4s$ and $4p$ orbitals on the Cu atoms and may be regarded as forming the valence $4sp$ "band" of the cluster. The 19 MO's—$13a_1^2$ to $16a_1^2$; $8b_1^2$ to $11b_1^2$; $12e^4$ to $17e^4$; $3b_2^2$ to $5b_2^2$; and $3a_2^2$ and $4a_2^2$—have predominantly d character and form the "d band" of the cluster. The ground state of Cu_5CO is also a ^2E state with the configuration

$$15a_1^2(\tilde{3}\sigma^2)16a_1^2(\tilde{4}\sigma^2)17a_1^2(\tilde{5}\sigma^2)\cdots 22a_1^2\cdots 12e^4(\tilde{1}\pi)\cdots 19e^3\cdots \ , \qquad (2)$$

where we show explicitly only the MO's derived from the valence "band" of the Cu_5 cluster and those derived from the valence levels of free CO. The $22a_1$ and $19e$ MO's are quite similar to the $17a_1$ and $18e$ orbitals of Cu_5. The CO derived levels are somewhat perturbed free CO orbitals; the notation $\tilde{n}\lambda$, in parentheses in Eq. (2), indicates the molecular origin of these levels.

In Table I, we give a Mulliken gross population analysis[21] for the MO's shown in Eq. (2) except for $\tilde{3}\sigma$ which is rather low lying and not involved in the bonding of CO to Cu_5. The population analysis is for $R(Cu_1-C)=3.75$ bohrs close to both the calculated and observed[10] Cu to C equilibrium distance. It is clear from Table I, that these levels are indeed rather similar to the orbitals of the component system CO or Cu_5, from which they are derived. Only two of the orbitals shown, $\tilde{5}\sigma$ and $19e$, are involved to any significant degree in the bonding of CO to Cu_5. The $\tilde{5}\sigma$ contributes a substantial donation of charge to Cu, mostly to $d\sigma$. The $19e$ level shows a reasonable amount of backbonding into the unoccupied CO $(2\pi^*)$ level. For the $19e^3$, this backbonding amounts to 0.08 electrons donated to $2\pi^*$. Of the orbitals which are not shown, only certain of the Cu_5 derived $d\sigma$ levels ($13a_1^2$ to $16a_1^2$ in Cu_5) contribute to the bonding. They serve to reduce the apparently very large σ donation arising from $\tilde{5}\sigma$. It is worthwhile to recall that in Hartree-Fock (HF) theory, the closed shell canonical HF orbitals do not have a unique physical significance. A set of orbitals yielding an identical wave function can be obtained from the canonical HF orbitals by a unitary transformation. Thus, only a sum over the closed shell orbitals, at least over those of the same symmetry, has proper physical significance.

In Table II, we examine the σ donation and π backdonation in a way in keeping with the idea expressed above. For Cu_5CO, we divide the total Mulliken gross population of the valence levels of CO into σ and π character. For the σ character the summation is over MO's belonging to the a_1 representation of C_{4v} and for π over MO's belonging to e. (The valence σ character is just the total σ population less 4 for the $1s$ cores.) The results are given for all Cu_1-C distances for which SCF calculations were performed. It is clear from Table II that the bonding of CO to Cu_5 may be characterized as arising from a σ donation of ~0.1 to 0.2e to Cu_5 and a roughly equal back donation into $CO(2\pi^*)$. As we have seen from Table I, most of this back donation arises from the $4sp$-like $18e$ valence orbital of Cu_5. In fact, we define the $2\pi^*$ occupation of CO in Cu_5CO as the π population minus 4 assuming a 1π occupation of 4. This characterization of the bonding of CO to a model of a Cu surface is reasonably similar to the bonding found from *ab initio* SCF calculations on transition-metal complexes, e.g., $Ni(CO)_4$.[22]

In Table II, we also give the interaction energy, E_{int} of CO with Cu_5. From a parabolic fit using the points at $R(Cu_1-C)=4.0$, 3.75, and 3.5, we find the equilibrium distance to be 3.88 bohrs; this is just outside of the error bounds of the value 3.6 ± 0.2 bohrs determined by a LEED analysis[10] for CO on Cu(100). The binding energy of CO with Cu_5, 0.45 eV, compares reasonably well with the experimental values obtained by Tracy[11] for CO on Cu(100) especially when the small, five atom, size of the Cu cluster is considered. Tracy reports binding energies of ~0.6 eV for $\frac{1}{2}$ monolayer coverage and ~0.7 eV extrapolated to zero coverage. It is interesting to note that for the ground state of the linear NiCO cluster,[23] the

TABLE I. Mulliken gross population analysis for some of the higher-lying MO's of Cu_5CO for $R(Cu_1-C)=3.75$ bohrs. Given are the levels derived from the 4σ, 5σ, and 1π levels of free CO and from the valence $4sp$ levels of the Cu_5 cluster, see Eq. (2). The Cu_5CO MO's are compared with those of the component system for which they are derived. The populations are decomposed into s, p, and d character; contributions less than 0.01 are neglected.

		Cu_5CO Cu_1	Cu_2	C	O	Component system (Cu_5 or CO)		C	O
$\tilde{4\sigma}$	s	···	···	0.28	0.23	4σ	s	0.21	0.24
	p	···	···	0.04	0.45		p	0.03	0.53
	d	···	···	···	···				
	tot	···	···	0.32	0.69		tot	0.23	0.77
$\tilde{5\sigma}$	s	0.05	..	0.34	0.01	5σ	s	0.57	−0.01
	p	···	···	0.32	0.15		p	0.33	0.10
	d	0.15	···	···	···				
	tot	0.20	···	0.66	0.16		tot	0.91	0.09
1π	p	···	···	0.25	0.74	1π	p	0.23	0.77
	d	···	···	···	···				
	tot	0.01	···	0.25	0.74		tot	0.23	0.77
								Cu_1	Cu_2
$19e$	s	···	0.16	···	···	$18e$	s	···	0.17
	p	0.14	0.05	0.02	0.01		p	0.13	0.05
	d	···	···	···	···		d	···	···
	tot	0.14	0.21	0.02	0.01		tot	0.13	0.22
$22a_1$	s	0.06	0.19	0.01	···	$17a_1$	s	0.18	0.17
	p	0.03	0.03	···	···		p	0.03	0.02
	d	···	0.01	···	···		d	···	0.01
	tot	0.09	0.23	0.01	···		tot	0.20	0.20

binding energy of CO to Ni is smaller, ~0.2 eV, than for CO to Cu_5. The σ donation in NiCO is comparable to that in Cu_5CO but the π^* backdonation is considerably smaller. It is smaller since the CO π system cannot, because of symmetry constraints in the linear cluster, interact with the metal $4p$ level.

TABLE II. Valence population of CO in Cu_5CO divided in σ and π character for various Cu_1-C distances, R. The interaction energy of CO with Cu_5 E_{int}, is also given.

R	CO(σ)	CO(π)	E_{int} (eV)
∞	6	4	0
4.00	5.90	4.09	−0.450
3.75	5.86	4.13	−0.448
3.50	5.81	4.17	−0.335
3.25	5.77	4.22	+0.021

This indicates that the π^* backdonation contributes appreciably to the total bond strength of CO to a metal surface.

All in all, the reasonable agreement of the equilibrium distance and binding energy obtained with the Cu_5CO cluster with experimental results for CO adsorbed on Cu(100) strongly suggests that the bonding in the cluster is rather close to that which occurs on a Cu surface.

IV. CO CORE HOLE STATE PROPERTIES

A. Electronic structure considerations

In this section, we present the properties of SCF wave functions for configurations of Cu_5CO where either the C or O $1s$ shell contains only one electron. Since the symmetry equivalence restrictions[20] were not used for these calculations, we may write the configurations as

$$1s^1 \cdots 19e_x^2 ne_y^1 \cdots , \quad (3)$$

where $1s$ denotes the singly occupied C_{1s} or O_{1s} shell and ne_y is the singly occupied MO of e_y symmetry: all other MO's are doubly occupied. For each core hole, O_{1s} or C_{1s}, we have found the two lowest states of the form of Eq. (3). For the wave functions and other properties of these states, we adapt the notation:

$$\text{Lowest: } \Psi_1 = 1s^1 19e_x^2 1e_y^1 \;,$$

$$\text{Second: } \Psi_2 = 1s^1 19e_x^2 2e_y^1 \;. \qquad (4)$$

We emphasize that Ψ_1 and Ψ_2 are obtained as separate solutions of the SCF equations.[12] For the open shell configuration, we have used an energy expression which corresponds to a weighted average of the singlet ($\frac{1}{4}$) and triplet ($\frac{3}{4}$) couplings of the $1s$ and ne_y open shells.[24] We shall show later, that for one state, Ψ_2, the singly occupied e_y MO, $2e_y$, is very similar to $19e_x$ while for the other state, Ψ_1, the $1e_y$ MO is dramatically different. Thus we have chosen to drop the symmetry equivalence restriction, since in this way states with different ne_y will be treated in a similar way within the average of configuration formalism; i.e., all states are two-open-shell states.

TABLE III. Mulliken gross and C—O overlap population analysis for selected MO's for CO hole states of Cu_5CO, see Eq. (4); $R(Cu_1-C)=3.75$ bohrs. The $2\pi^*$ MO of free CO, see Eq. (5), is included for comparison with the Cu_5CO $1e_y$ MO. The gross populations are decomposed into s, p, and d character; populations less than 0.01 are neglected.

State	Orbital		Cu_1	Cu_2	C	O	C—O
$\Psi_1(O_{1s}$ hole)	$19e_x$	s	· · ·	0.15	· · ·	· · ·	· · ·
		p	0.16	0.05	0.04	· · ·	· · ·
		d	· · ·	· · ·	· · ·	· · ·	· · ·
		tot	0.16	0.20	0.04	· · ·	−0.01
	$1e_y$	s	· · ·	· · ·	· · ·	· · ·	· · ·
		p	0.01	· · ·	0.93	0.04	· · ·
		d	0.01	· · ·	· · ·	· · ·	· · ·
		tot	0.02	· · ·	0.93	0.04	−0.36
	$CO(2\pi^*)$[a]	p	· · ·	· · ·	0.95	0.05	−0.38
$\Psi_2(O_{1s}$ hole)		s	· · ·	0.14	· · ·	· · ·	· · ·
$E_2-E_1=5.62$ eV	$19e_x$	p	0.17	0.04	0.06	0.01	· · ·
		d	0.01	· · ·	· · ·	· · ·	· · ·
		tot	0.17	0.19	0.06	0.01	−0.04
		s	· · ·	0.15	· · ·	· · ·	· · ·
	$2e_y$	p	0.15	0.04	0.07	0.01	· · ·
		d	0.01	· · ·	· · ·	· · ·	· · ·
		tot	0.16	0.19	0.07	0.01	−0.05
$\Psi_1(C_{1s}$ hole)		s	· · ·	0.15	· · ·	· · ·	· · ·
	$19e_x$	p	0.15	0.05	0.02	0.02	· · ·
		d	· · ·	· · ·	· · ·	· · ·	· · ·
		tot	0.15	0.20	0.02	0.02	−0.01
		s	· · ·	· · ·	· · ·	· · ·	· · ·
	$1e_y$	p	· · ·	· · ·	0.66	0.33	· · ·
		d	0.01	· · ·	· · ·	· · ·	· · ·
		tot	· · ·	· · ·	0.66	0.33	−0.45
	$CO(2\pi^*)$[b]	p	· · ·	· · ·	0.68	0.32	−0.45
$\Psi_2(C_{1s}$ hole)		s	· · ·	0.14	· · ·	· · ·	· · ·
$E_2-E_1=6.77$ eV	$19e_x$	p	0.23	0.05	0.01	0.01	· · ·
		d	· · ·	· · ·	· · ·	· · ·	· · ·
		tot	0.23	0.19	0.01	0.01	−0.02
		s	· · ·	0.15	· · ·	· · ·	· · ·
	$2e_y$	p	0.22	0.04	0.01	0.01	· · ·
		d	· · ·	· · ·	· · ·	· · ·	· · ·
		tot	0.22	0.19	0.01	0.01	−0.02

[a]Calculated for free CO with an O_{1s} hole. [b]Calculated for free CO with a C_{1s} hole.

The properties of these two states are characterized by the data given in Tables III and IV. For both tables, the results are for the representative distance $R(\mathrm{Cu_I{-}C}) = 3.75$ bohrs. In Table III, we give Mulliken population analyses for the $19e_x$ and ne_y MO's including the C–O overlap population.[21] We also give the energy separation, $\Delta E = E_2 - E_1$, between the two states. This separation is ~6 eV which is close to the width observed in the XPS spectra for CO on Cu [both Cu(100) and polycrystalline Cu films] of the C_{1s} (Refs. 2 and 25) and O_{1s} (Refs. 25 and 26) levels. For all four states, Ψ_1 and Ψ_2 for O_{1s} and C_{1s} holes, the $19e_x$ MO resembles the bare cluster $18e$ or ground state Cu_5CO $19e$ MO (see Table I). It is a predominantly Cu $4sp$ level and the CO contribution is always small; the largest is 6% for $\Psi_2(O_{1s}$ hole). The $1e_y$ MO for Ψ_1 (O_{1s} hole) or for $\Psi_1(C_{1s}$ hole) is essentially a pure CO level and the large negative C–O overlap population shows that it is clearly antibonding between C and O. Also shown in Table III are population analyses for the $2\pi^*$ MO for free CO with O_{1s} or C_{1s} holes:

$$1\sigma^1(O_{1s})2\sigma^2 3\sigma^2 4\sigma^2 5\sigma^2 1\pi^4 2\pi^1$$

or

$$1\sigma^2 2\sigma^1(C_{1s})3\sigma^2 4\sigma^2 5\sigma^2 1\pi^4 2\pi^1 \ . \quad (5)$$

The similarity between the free CO $2\pi^*$ for the appropriate core hole and the $1e_y$ cluster MO is striking. Clearly $1e_y$ is properly described as $2\pi^*$. The $2e_y$ MO, again for either $\Psi_2(O_{1s}$ hole) or $\Psi_2(C_{1s}$ hole), is very similar to the $19e_y$ MO. Thus to a rather good approximation, the conformations of Eq. (4) may be written

$$\Psi_1 = 1s^1 19e^2 2\pi^{*1} \ , \quad \Psi_2 = 1s^1 19e^3 \ . \quad (6)$$

The state Ψ_2 would often be described as the "normal" hole state since its configuration, Eq. (6), most nearly resembles that of the ground state, Eq. (2), with a single core electron removed. The state Ψ_1 would often be described as a "shake" state[27,28] since its configuration is one in which the $1s$ electron has been ionized and a second electron has been moved or "excited" from $19e$ to $2\pi^*$. In this case, the shake state lies ~6 eV *below* the normal state. This is in contrast to the usual notion that shake states have a higher energy than the normal state because of the energy required to excite the second electron. However, for Cu_5CO, the energy gained by filling the $2\pi^*$ level (in the presence of a core hole) is greater than that paid by removing it from Cu_5. The energy gained by adding an electron to CO^+ with a C_{1s} hole is, in the equivalent core mode,[29] the same as the ionization potential, IP, of NO, ~10 eV. The energy paid can be estimated from the orbital energy of the

TABLE IV. Valence population of CO in Cu_5CO divided into σ and π character for the ground and various CO core hole states; $R(\mathrm{Cu_I{-}C}) = 3.75$ bohrs. The total charge on CO, Q, is also given.

State	CO(σ)	CO(π)	Q
Ground state	5.86	4.13	−0.01
$\Psi_1(O_{1s}$ hole)	5.88	5.09	+0.03
$\Psi_2(O_{1s}$ hole)	6.00	4.37	+0.63
$\Psi_1(C_{1s}$ hole)	5.85	5.09	+0.06
$\Psi_2(C_{1s}$ hole)	5.91	4.30	+0.79

$19e$(MO) in Cu_5CO, $\epsilon(19e) \sim 5$ eV. In band-structure terminology, the presence of a core hole has pulled $2\pi^*$ below E_F.[3–5] Thus, we can reasonably describe Ψ_1 as a shake-down state.

In Table IV, we give the valence population of CO decomposed into σ and π character in a similar way as described above for the ground state. For Ψ_1, for either a C_{1s} or O_{1s} hole, the π population of $5.1e$ indicates a $2\pi^*$ occupation of ~1 electron. (No particular significance should be given to the population of 1.1 as opposed to 1 since a Mulliken population analysis gives only a qualitative guide to the distribution of charge. Artifacts, especially for the extended basis sets used in this work, can be expected to arise.[19] The σ donation is approximately the same, $\sim 0.1e$, for the shakedown hole states as for the cluster ground state. Clearly these states are the MO analogs of the fully screened final states described by SG.[3–5] For the "normal" hole states, Ψ_2 the $2\pi^*$ population has also increased over that for the ground state but is much smaller than the Ψ_1 $2\pi^*$ population. There also appears to be some reduction of the donation in Ψ_2 compared to the ground state so that there may be a small σ contribution to the screening of the core hole. Although, this population decomposition does suggest some σ and π^* screening of the core hole, it is reasonable to think of at least part of this as being more like a polarization of charge on Cu_5 rather than an actual charge transfer from Cu_5 to CO. The apparent charge transfer in the Ψ_2 states is, in part, an artifact of the population analysis. If we were to estimate the many-electron overlap integral $\langle \Psi_1 | \Psi_2 \rangle$ from the populations of $2\pi^*$ given in Table IV, we would expect it to be reasonably large, ~0.5. However, as we shall show below the overlap is, in fact, rather small. Clearly then, the normal hole states, Ψ_2 are the MO analogs of the SG "unscreened" final states.

B. Relative XPS intensities of the hole states

It is necessary to know the relative photoionization intensities for the two final hole states, Ψ_1 and Ψ_2, in order to make a meaningful comparison with the XPS spectra for CO on Cu. It is not sufficient that the "shakedown" states lie below the "normal" hole states. Unless both kinds of states have substantial intensity, they will not be easily observed and, thus, cannot be the origin of the broad XPS structures.[2,25,26] In order to compute the relative intensities, we use the sudden approximation (SA).[27] This approximation is suitable for the high energy, ~1 keV, CO core electrons ionized by Mg or Al $K\alpha$ radiation. For the present case, we require the integrals I_i,

$$I_i = \langle \Psi_{\text{final},i} | \Psi^{-1s}_{\text{initial}} \rangle \ , \tag{7}$$

where $\Psi_{\text{final},i}$ is one of the SCF wave functions of Eq. (4) and $\Psi^{-1s}_{\text{initial}}$ is the ground-state wave function, Eq. (2), with a CO $1s$ electron removed. It is important to emphasize that I_i is a many-electron integral between Slater determinants constructed from two different (nonorthogonal) sets of MO's, the final-ion-state SCF orbitals for Ψ_{final} and the ground-state SCF orbitals for $\Psi^{-1s}_{\text{initial}}$.[30] The relative probability P_i, of a photoionization event leading to Ψ_i is

$$P_1 = 3I_1^2 \ , \quad P_2 = I_2^2 \ . \tag{8}$$

The factor 3 is required because any one of the 3 $19e$ electrons can be excited to an appropriate $1e(2\pi^*)$ MO.[31] In order to evaluate I_i, we have chosen to use wave functions in which the open shells have an explicit coupling to either singlet or triplet spin states, see Eq. (4). Either choice leads to the same value for I_i. The resultant P_i are the sum of the intensities for ionization leading to either $\Psi_{\text{final},i}$ (singlet) or to $\Psi_{\text{final},i}$ (triplet). We consider this sum of intensities, P_i, since the total spins of the various states of Cu_5CO are clearly cluster artifacts. However, the fact that the $1e_y(2\pi^*)$ electron and $1s$ hole for the shakedown state Ψ_1, may couple to form singlets and triplets is a real physical effect. Possible consequences of this coupling will be discussed below.

In Table V, we list values of P_i for O_{1s} and C_{1s} core holes for $R(Cu_I-C) = 3.75$ bohrs which is close to the equilibrium Cu–C distance and for $R(Cu_I-C) = 3.25$ bohrs where the distance has been shortened somewhat. Clearly, the "shakedown" state always has substantial intensity. Even in the case where P_1 is smallest, C_{1s} hole at $R(Cu_I-C) = 3.75$, it is still greater than 20% of the intensity of P_2. The intensity of P_1 increases and that of P_2 decreases as the Cu_I–C distance is decreased. This is consistent with the interpretation that the intensity of P_1 has a major origin due to the π^* backbonding in

TABLE V. Relative intensities, P_i, for the CO core hole states of Cu_5CO computed in the sudden approximation, see Eqs. (7) and (8). The many-electron overlap integral between the shakedown and normal final hole states, $\langle \Psi_1 | \Psi_2 \rangle$, is also given.

Hole	$R(Cu_I-C)$ bohrs	P_1	P_2	P_1/P_2	$\langle \Psi_1/\Psi_2 \rangle$
O_{1s}	3.75	0.16	0.38	0.42	0.13
O_{1s}	3.25	0.29	0.16	1.82	0.16
C_{1s}	3.75	0.12	0.54	0.22	0.07
C_{1s}	3.25	0.21	0.43	0.48	0.09

the initial, unionized, state. As may be seen in Table II, this backbonding increases as the Cu_I–C distance decreases. The large values for the ratio P_1/P_2, particularly for $R(Cu_I-C) = 3.25$, are consistent with the observed XPS spectra for the C_{1s} and O_{1s} levels for CO adsorbed on a Cu surface.[2,25,26] They indicate that the considerable intensity will be observed for both Ψ_1 and Ψ_2 which are separated by about 6 eV and, indeed, the XPS spectra for CO on Cu show broad peaks over a comparable energy range. Since the cluster clearly gives a limited representation of the surface valence *sp* band, it seems reasonable to consider modest variations of the cluster Cu_I–C distance about equilibrium in order to obtain a ratio P_1/P_2 which, in some sense, compensates for this limitation.[6,7] Values of P_1/P_2 computed for $R(Cu_I-C)$ near 3.25 do compare reasonably with experiment.

For CO, using the same C and O basis sets as in the cluster, the relative intensity for the normal O_{1s} hole is 0.76 and for the normal C_{1s} hole 0.81. The remaining intensity, 24% for O_{1s} and 19% for C_{1s}, goes to shakeup and shakeoff states.[28,30,32]

We present now an analysis to obtain a better understanding of the origin of the intensity P_1 and of how the shakedown state Ψ_1 gains intensity at the expense of the normal state Ψ_2. In this analysis, we consider the contribution to P_i from the highest-lying e orbitals. These are the MO's denoted $19e$ ($19e_x$ and $19e_y$), $1e_y$ and $2e_y$ in Eqs. (2) and (4). We define the following integrals:

$$\begin{aligned} i_l(x) &= \langle 19e_x(\text{g.s.}) | 19e_x(\Psi_l) \rangle \ , \\ i_l(y) &= \langle 19e_y(g.s.) | le_y(\Psi_l) \rangle \ . \end{aligned} \tag{9}$$

Here the subscript l denotes the final ionic state (1 for the shakedown state and 2 for the normal state); $19e$(g.s.) is the SCF orbital determined for the ground state, Eq. (2); and $19e_x(\Psi_l)$ and $1e_y(\Psi_l)$ are SCF orbitals determined for the final states of Eq. (4). The partial contributions to P, denoted $\tilde{P}$, from these integrals are[30]

$$\tilde{P}_1 = 3|i_1(x)|^4|i_1(y)|^2 \ , \ \ \tilde{P}_2 = |i_2(x)|^4|i_2(y)|^2 \ . \qquad (10)$$

Values for the quantities in Eqs. (9) and (10) for R(Cu–C) = 3.75 bohrs are given in Table VI. For the shakedown state, for both O_{1s} or C_{1s} holes, $i_1(x)$ is nearly 1 indicating that $19e$(g.s.) and $19e_x(\Psi_1)$ are very similar MO's. This is also suggested by the population analysis in Tables I and III. The key factor in determining $\tilde{P}_1$ (and also P_1) is $i_1(y)$. This integral is between an MO which is predominantly Cu_5 with some $2\pi^*$ backbonding character, $19e$(g.s.), and one which is essentially $2\pi^*$, $1e_y(\Psi_1)$. This integral is different from zero because the $19e$(g.s.)MO contains $2\pi^*$ backbonding character. If it were a pure Cu_5 orbital, $i_1(y)$ would be very much smaller. Indeed, it is not large compared to 1 especially considering that it enters the expression for $\tilde{P}_1$ as $|i_1(y)|^2$. It is, however, sufficiently large to lead to substantial value for $\tilde{P}_1$ compared to $\tilde{P}_2$. For the second, normal hole, state, $i_2(x) \approx i_2(y)$ indicating that the $19e_x(\Psi_2)$ and $2e_y(\Psi_2)$ MO's are quite similar. This is gratifying since it means that the effect of dropping the symmetry equivalence restriction[20] for this ionic state is not great; compare Eqs. (4) and (6) for Ψ_2. The values of $i_2(x)$ and $i_2(y)$ are somewhat less than 1, ~0.9–0.95, but this is sufficient to reduce $\tilde{P}_2$ to a value substantially less than 1; see Eq. (10). These integrals are reduced from 1 because the $19e_x$ and $19e_y$ MO's for Ψ_2 are somewhat polarized toward CO in response to the presence of the CO core hole. This polarization is seen in the population analysis as a shift of charge away from Cu_2 to Cu_1 for $19e(\Psi_2)$ compared to $19e$(g.s.); see Tables I and II. It is also seen in the change in the $\langle Z \rangle$ for $19e$ between the ground state and Ψ_2. The values of $\tilde{P}_i$ are larger than those for P_i; this is necessary since the orbitals not considered in $\tilde{P}_1$ relax in the final states and lead to a smaller value for the all electron intensity, P_i.[30] However, the relative values of $\tilde{P}_i$ are rather similar to those of P_i.

This analysis clearly shows that the π^* backbonding in the $19e$ MO of the cluster ground state is the primary reason that the intensity of the shakedown state, P_1, is reasonably large. It also shows that the polarization of the $19e$ MO in the normal final states, Ψ_2, leads to a substantial loss of intensity for these states.

The many-electron overlap integrals between the shakedown and normal final states, $\langle \Psi_1 | \Psi_2 \rangle$, are, as may be seen from Table V, small. As we mentioned above, they are much smaller than one would expect from the CO(π) populations of Ψ_1 and Ψ_2 shown in Table IV; however, they are certainly not zero. One way to estimate the effect of the nonzero overlap on the relative SA intensities P_i is to construct a Ψ_2' orthogonal to Ψ_1 by Schmidt orthogonalization,

$$\Psi_2' = (\Psi_2 - \alpha\Psi_1)(1-\alpha^2)^{-1/2} \ , \ \ \alpha = \langle \Psi_1 | \Psi_2 \rangle \ . \qquad (11)$$

The SA intensity P_2' may then be evaluated for Ψ_2'. If this is done, for example, for the O_{1s} hole for R(Cu–C) = 3.75 bohrs, $P_2' = 0.35$, 10% smaller than P_2. Thus, the lack of orthogonality between Ψ_1 and Ψ_2 will affect somewhat the values of P_1 and P_2. However, it will not, for the small values of the overlap that we find here, affect the general features of the intensity distribution shown in Table V.

TABLE VI. Analysis of the contributions of the highest-lying MO's of e symmetry to the relative intensities of the CO core hole states of Cu_5CO for $R(Cu_1\text{–}C) = 3.75$ bohrs. The integrals over the MO's are denoted by $i_l(x)$ and $i_l(y)$ and the intensity contributions by $\tilde{P}_l$; see Eqs. (9) and (10) for definitions of these quantities.

Hole	$i_1(x)$	$i_1(y)$	$\tilde{P}_1$	$i_2(x)$	$i_2(y)$	$\tilde{P}_2$	$\tilde{P}_1/\tilde{P}_2$
O_{1s}	0.99	0.26	0.20	0.91	0.90	0.56	0.36
C_{1s}	0.99	0.21	0.13	0.95	0.95	0.75	0.17

C. Comparison with XPS spectra for CO on Cu

As we have discussed above the energy separation and the intensity distribution between the shakedown and normal final states is consistent with the observed width and intensity distribution for the CO core level XPS spectra for CO on Cu. It is not possible for us, however, to make a comparison between our cluster results and the detailed shape of the XPS spectra. We have computed two sharp peaks while broad continuous spectra are observed. In Cu_5CO, there is only one level, $19e$, which may couple or interact with CO($2\pi^*$). On the Cu surface, there are a range of levels in the sp band which can interact in this way.[3–5] The effect of this will be to broaden the two single lines which we have computed in a way which reflects the nature of the valence sp band at the Cu surface. Furthermore, we have not considered here shake states which arise from a Cu $d\pi$ electron being transferred to CO($2\pi^*$). Such states have been investigated for a linear NiCO cluster.[33] It was found that these are also shakedown states but that they have rather less intensity than the valence *sp* to $2\pi^*$ shake states considered here. However, the effect of such $d\pi$ to $2\pi^*$ states will be to add intensity to the shake (or fully screened) XPS region and to further broaden it.

Finally, we have, in the shakedown state, Ψ_1, neglected the spin coupling of the $2\pi^*$ electron with the core hole. For free CO with the configurations of Eq. (5), we have obtained SCF wave functions for both the singlet and triplet couplings of $1s$ with $2\pi^*$. For the C_{1s} hole, the energy difference of these two states is $\Delta E_{st} = 1.4$ eV; for an O_{1s} hole, $\Delta E_{st} = 0.3$ eV. The larger ΔE_{st} for the C_{1s} hole is due to the fact that $2\pi^*$ for both C_{1s} and O_{1s} hole states has its largest density about the C atom; see Table III. Clearly the exchange integral $K(1s, 2\pi^*)$ will be larger for C_{1s} than for O_{1s}. Since $\Delta E_{st} \approx 2K(1s, 2\pi^*)$, it is larger for C_{1s}. It is worth noting that, for CO on Cu, the C_{1s} XPS spectra is somewhat broader than that for O_{1s} and that it has a somewhat more complex structure.[26] It is quite possible that the greater importance of the $1s$-hole$-2\pi^*$ electron coupling for C_{1s} is, at least in part, responsible for these observed differences.

We have not yet considered the absolute values of our calculated CO core level ionization potentials, E_{IP}. These IP's for Cu_5CO and for free CO, are compared with experimental values in Table VII. The calculated IP's are obtained by taking differences of the total SCF energies of the initial ground state and the final ionic state.[12] $E_{IP}(\text{calc}) = E_{SCF}(\text{ground state}) - E_{SCF}(\text{core-hole ion})$. We consider first the results for free CO. Here, the calculated and experimental values agree to within about 3 eV. The errors in the calculation will arise principally because a limited basis set is used; because of different correlation errors for the ground state and ionic states; and from relativisitic corrections ($\sim$0.4 eV for O_{1s} and smaller for C_{1s}).[28,34] In Table VII,[35] we have included calculated IP's for CO which use a large basis set and give Hartree-Fock limit results.[34] It is clear that the largest part of the error of the CO IP's calculated with the present basis, $\sim$2 eV, is due to limitations of this basis set.

For Cu_5CO, the calculated IP's given in Table VII are those for ionization to the lowest shakedown, state Ψ_1 for $R(Cu_1{-}C) = 3.75$ bohrs. (However, between $R = 3.75$ and 3.25, the change of the IP's is quite small; less than 0.2 eV.) For CO on Cu(100), the experimental values are taken as the position of the first, lowest apparent binding energy, maximum in the XPS spectra. These values measured relative to E_F are adjusted by the Cu work function to give IP's relative to vacuum in order to have an appropriate comparison with the IP's calculated for Cu_5CO. The agreement between the IP's for Cu_5CO and CO on Cu(100) is very good. We may estimate the correction for the limitations in the basis set by assuming that they lead to the same error in the calculated IP's for Cu_5CO as for free CO. Making this correction does not significantly change the quality of agreement between theory and experiment: the differences, corrected in this way, are still $\sim$1 eV.

This agreement gives strong support to our assignment of the lowest observed levels in the CO on Cu XPS spectra to shakedown states which have large intensity. It also demonstrates that a rather small metal cluster of five atoms is sufficiently large to give absolute IP's in remarkable agreement with the core level XPS IP's for CO chemisorbed on a Cu surface. At first, this would seem rather surprising since the cluster is much too small to fully include the final state relaxation (response) of the metal to the CO core hole. However, the response that we have neglected, that due to distant metal atoms, is most likely to occur on a time scale which is long compared to the time required for the high-energy photoelectron to be emitted.[36] Thus, it will contribute to the tail to lower binding energy which is observed in the XPS spectra[2,25,26]; however, it is not very likely that it will greatly shift the position of the peak maximum.

TABLE VII. Theoretical and experimental ionization potentials, in eV, for the free CO molecule, Cu_5CO and CO on Cu(100). For free CO, the Hartree-Fock limit results, see Ref. 34, are given in parenthesis. For Cu_5CO, the IP's are for $R(Cu_1{-}C) = 3.75$ bohrs.

Hole	Expt[a]	CO Theory	Δ(Expt − Theory)	CO on Cu(100) Expt[b]	Cu_5CO Theory	(Expt − Theory)
C_{1s}	296.2	298.7	−2.5	292.1	292.8	−0.7
		(296.9)	(−0.7)			
O_{1s}	542.3	539.1	+3.2	539.1	538.0	+1.1
		(541.6)	(+0.7)			

[a]See Ref. 35.
[b]Corrected for the vacuum level as the zero of energy, see Ref. 26.

V. CONCLUSIONS

We have used *ab initio* SCF wave functions for a Cu_5CO cluster to model the interaction and x-ray photoionization processes for CO adsorbed on a Cu surface. We have shown that these wave functions lead to reasonable results for properties related to the interaction in the ground state; in particular for the Cu to CO bond distance and for the chemisorption bond strength. Further, the absolute values of the cluster IP's for CO core ionization are in excellent agreement with the observed XPS IP's for CO on Cu(100). This is strong evidence that the present theoretical approach, including both choice of cluster and the use of SCF wave functions, provides quite a good (realistic) representation for the behavior of CO on a real Cu surface.

This is quite important in itself. However, it also means that cluster results should be reliable as well for the interpretation of the origin of the broad and complex structure of the adsorbate core level XPS spectra observed for CO on Cu and for other weakly bound adsorbate-metal systems.[2] This interpretation is, indeed, the major objective of this work. Our results lead to the conclusion that the broad spectra arises from the fact that two distinctly different kinds of final, core hole, states exist. Each kind has substantial intensity in the XPS spectra of CO on Cu and, most likely, for other weakly chemisorbed molecules.[6,7] On a real surface, there will be a large number (band) of final states of each kind.[3–5] With our Cu_5CO cluster, we have represented each of these two bands by a single state. The lower state can be described as a "shakedown" state where the metal has contributed an electron from a valence $4sp$ level to the $CO(2\pi^*)$ in order to screen the CO core hole. The second state, $\sim$6 eV higher in energy, is a "normal" single hole state where the CO core hole is not substantially screened. The relative XPS intensity of these two states, computed in the sudden approximation, is shown to depend very strongly on the fact that there is significant metal valence ($4sp$) to $2\pi^*$ backbonding in the ground state of the system. The separation of these two states and their relative intensities for Cu to CO distances near equilibrium separation are qualitatively consistent with the observed XPS spectra for CO on Cu. We have also considered the spin coupling of the $2\pi^*$ electron and core hole and conclude that the effect of this coupling will be negligible for an O_{1s} hole and may lead to a broadening of $\sim$1.5 eV for the C_{1s} spectra. This hole-electron coupling effect, together with the fact that the separation of the shakedown and normal states is $\sim$1 eV larger for C_{1s} than O_{1s} holes, is consistent with the observation that the XPS C_{1s} spectra is broader than that for O_{1s}.

Our conclusion concerning the origin of the adsorbate core level spectra is similar to the one arrived at by Schönhammer and Gunnarsson[3–5] whose work is based on the use of a parametrized Anderson-type Hamiltonian. They were able, with this Hamiltonian, to take explicit account of the metal band structure but had to use, and in certain cases to adjust, empirical parameters to represent the CO–Cu surface interaction and the position of the $2\pi^*$ level. In our work, by contrast, we have an obviously very limited representation of the surface band structure with the Cu_5CO cluster, but we have treated the interaction and energetics without empirical or adjustable parameters. If any further evidence were needed for the correctness of the interpretation of the role of screened (shakedown) and unscreened (normal) states in the XPS spectra, the similarity of our conclusions with these of SG should provide it. We have used entirely different theoretical approaches which emphasize different aspects of the problem, yet we, both, come to the same physical model.

ACKNOWLEDGMENT

One of us (PSB) wishes to express his gratitude to Professor J. Ladik for his kind hospitality and to the Alexander von Humboldt Foundation for the U.S. Senior Scientist Award which made his stay in Erlangen possible.

[1]See, for example, K. Siegbahn, C. Nordling, A. Fahlman, R. Nordberg, K. Hamrin, J. Hedman, G. Johansson, T. Bergmark, S. Karlsson, I. Lindgren, and B. Lindberg, Nova Acta Regiae Soc. Sci. Ups. 20, 1 (1967).
[2]J. C. Fuggle, E. Umbach, D. Menzel, C. Wandelt, and C. R. Brundle, Solid State Commun. 27, 65 (1978).
[3]K. Schönhammer and O. Gunnarsson, Solid State Commun. 23, 691 (1977); 26, 399 (1978).
[4]O. Gunnarsson and K. Schönhammer, Phys. Rev. Lett. 41, 1608 (1978).
[5]O. Gunnarsson and K. Schönhammer, Surf. Sci. 80, 471 (1979).
[6]P. S. Bagus and K. Hermann, Surf. Sci. 89, 588 (1979).
[7]K. Hermann and P. S. Bagus, Solid State Commun. (in press).
[8]P. S. Bagus, K. Hermann, C. R. Brundle, and D. Menzel, J. Electron Spectrosc. Relat. Phenom. (in press); K. Hermann, P. S. Bagus, C. R. Brundle, and D. Menzel (unpublished).
[9]S. Andersson, Surf. Sci. 89, 477 (1979).
[10]S. Andersson and J. B. Pendry, Phys. Rev. Lett. 43, 363 (1979).
[11]J. C. Tracy, J. Chem. Phys. 56, 2748 (1972).
[12]P. S. Bagus, Phys. Rev. 139, A619 (1965).
[13]C. R. Brundle (private communication).
[14]P. S. Bagus and M. Seel (unpublished).

[15]R. W. G. Wyckoff, *Crystal Structures*, 2nd ed. (Interscience, New York, 1964), Vol. II.
[16]J. Ladell, B. Post, and I. Fankuchen, Acta Crystallogr. 5, 795 (1952).
[17]G. Herzberg, *Spectra of Diatomic Molecules* (Van Nostrand, New York, 1950).
[18]For a complete description of the basis sets for Cu, C, and O, see Ref. 14.
[19]For a discussion of the basis set SCF procedure and of the notation and accuracy of various basis sets see H. F. Schaefer, III, *The Electronic Structure of Atoms and Molecules* (Addision-Wesley, Reading, Mass., 1972).
[20]R. K. Nesbet, Proc. R. Soc. London Ser. A 230, 312 (1955).
[21]R. S. Mulliken, J. Chem. Phys. 23, 1833, 1841, 2338, 2343 (1955).
[22]J. Demuynck and A. Veillard, Theor. Chim. Acta 28, 241 (1973).
[23]K. Hermann and P. S. Bagus, Phys. Rev. B 16, 4195 (1977).
[24]J. C. Slater, *Quantum Theory of Atomic Structure* (McGraw-Hill, New York, 1960), Vol. I.
[25]C. R. Brundle and K. Wandelt, in *Proceedings of the 7th International Vacuum Congress and 3rd International Conference Solid Surfaces, Vienna, 1977*, edited by R. Drobrozemsky *et al.* (Pergamon, Oxford, 1978), p. 1171.
[26]C. R. Brundle (private communication).
[27]T. Åberg, Phys. Rev. 156, 35 (1967).
[28]D. A. Shirley, Adv. Chem. Phys. 23, 86 (1973).
[29]W. L. Jolly, in *Electron Spectroscopy*, edited by D. A. Shirley (North-Holland, New York, 1972), p. 629.
[30]For a discussion of the evaluation of the integral in Eq. (7) and further references, see P. S. Bagus, H. Schrenk, D. W. Davis, and D. A. Shirley, Phys. Rev. A 9, 1090 (1974).
[31]T. A. Carlson, C. W. Nestor, Jr., and T. C. Tucker, Phys. Rev. 169, 27 (1968).
[32]K. Siegbahn, C. Nordling, G. Johansson, J. Hedman, P. F. Hedén, K. Hamrin, U. Gelius, T. Bergmark, L. O. Werme, R. Manne, and Y. Baer, *ESCA Applied To Free Molecules* (North-Holland, Amsterdam, 1969).
[33]P. S. Bagus and K. Herman (unpublished results).
[34]P. S. Bagus, in *Proceedings of the International Symposium on X-ray Spectra and Electronic Structure of Matter*, edited by A. Faessler and H. Wiech (Frank, München, 1973), Vol. I, p. 256.
[35]T. D. Thomas, J. Chem. Phys. 53, 1744 (1970).
[36]J. W. Gadzuk, Phys. Rev. B 20, 515 (1979).